Magnetically tunable hollow-core anti-resonant fiber polarizer*

LIANG Hu (梁鹄)**, **ZHAO Xiao-ming** (赵小明), **LI Mao-chun** (李茂春), **LIU Bo-han** (刘伯晗), **YU Jie** (于杰), **and MA Jun** (马骏)

Tianjin Navigation Instruments Research Institute, Tianjin 300131, China

(Received 18 June 2020; Revised 20 June 2020)

An in-line high efficient polarizer, composed of magnetic-ionic-liquid-adorned (MIL-adorned) hollow-core anti-resonant fiber (HARF), is theoretically proposed and experimentally demonstrated. The protocol is based on the selective conversion of polarization mode into leaky mode and attenuates quickly in MIL and the polarizer is featured by the magnetically tunable polarization extinction ratio (*PER*) and the thermally controllable operation bandwidth.

Document code: A **Article ID:** 1673-1905(2021)01-0012-6

DOI https://doi.org/10.1007/s11801-021-0105-7

In addition to having the advantages of high extinction ratio, low insertion loss and sufficient compatibility, all-fiber polarizer could enhance the integrating and reusability of optical fiber communication and sensing system, such as fiber-optic gyroscope[1]. Prevalent fiber-optic polarizers are produced by modifying fiber to be asymmetric waveguide structure, such as indium-coated D-shaped-fiber[2], thin metal-deposited side-polished single mode fiber (SMF)[3], long period fiber grating written on photonic crystal fiber (PCF)[4], hollow-core photonic bandgap fiber with partial collapse of air holes in the cladding[5], ultraviolet (UV) inscribed 45° tilted grating in polarization maintaining fiber[6], etc. Moreover, by decorating the side of fiber with Au thin film[7] or the fiber tip with metal nano-grid[8], high efficient fiber polarizers could be derived as well. More delightfully, the holey cladding of PCFs affords new degrees of freedom in polarizer design[9,10], enhancing the stability and simplifying the structure of the device.

Based on the operating principle of anti-resonant reflecting optical waveguide (ARROW)[11], a sort of hollow-core fiber (HCF) (named as hollow-core anti-resonant fiber (HARF) in this paper) composed by one layer of six to eight untouched thin tubes has become a research frontier in the field of fiber optics with extraordinary optical performance in the aspect of low loss, broadband and high mode quality[12,13], and the vigorous area of research involving HARF ranges from their applications in high average power pulse delivery[14,15], nonlinear optics[16], mid-infrared fiber gas laser[17], and short haul data communications[18]. In addition, the typical core size of HARF can provide an excellent platform to develop fiber-based optofluidic devices[19]. However, to our knowledge, few research works have been focused on the HARF-based polarizer.

In this letter, we demonstrate a novel magnetically tunable fiber polarizer, constituted by an MIL-adorned HARF. By introducing the perturbance of refractive index (RI) contrast to modulate the single-path Fresnel transmission in HARF, the energy of one polarization mode leaks out into the liquid, while the orthogonal polarization mode is hardly influenced and can propagate along the fiber freely. The polarization extinction ratio (*PER*) of the device can be magnetically tunable due to the controllable optical absorption and scattering coefficients of MIL under the applied magnetic field.

Fig.1 illustrates the schematic diagram of the proposed HARF-based polarizer configuration, capable of damping *Y*-polarization mode into MIL. The cross section of the HARF employed in the experiment is presented in the inset of Fig.1, the HARF is fabricated by six untouched tubes embracing the hollow core, and the fiber structural parameters would be introduced in experimental section. According to the mechanism of light guidance in HARF, four physical origins including multi-path interference caused by Fresnel reflection (ARROW), glass wall shape, near-grazing incidence, and single-path Fresnel transmission are responsible for the light confinement[20,21]. Obviously, the first three origins rest with the essential properties of the fiber structure, which would not be influenced by the contrived perturbation inside the tube. However, the RI contrast between the silica tube and MIL would most likely transform the conditions of Fresnel transmission on the interface, which is significant for further revealing the inexplicit guidance mechanism of HARF.

* This work has been supported by the Youth Innovation Fund of Tianjin Navigation Instruments Research Institute (No.QN-19-02-GX).
** E-mail: ymirlh@163.com

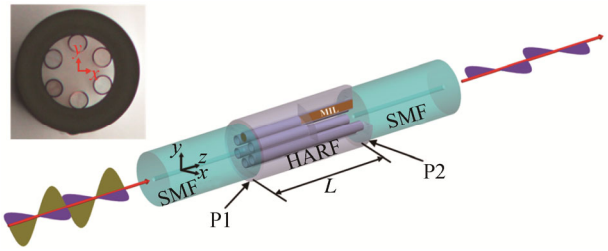

Fig.1 Schematic diagram of the proposed HARF polarizer

Fig.1 illustrates the schematic diagram of the proposed HARF-based polarizer configuration, capable of damping *Y*-polarization mode into MIL. The cross section of the HARF employed in the experiment is presented in the inset of Fig.1, the HARF is fabricated by six untouched tubes embracing the hollow core, and the fiber structural parameters would be introduced in experimental section. According to the mechanism of light guidance in HARF, four physical origins including multi-path interference caused by Fresnel reflection (ARROW), glass wall shape, near-grazing incidence, and single-path Fresnel transmission are responsible for the light confinement[20,21]. Obviously, the first three origins rest with the essential properties of the fiber structure, which would not be influenced by the contrived perturbation inside the tube. However, the RI contrast between the silica tube and MIL would most likely transform the conditions of Fresnel transmission on the interface, which is significant for further revealing the inexplicit guidance mechanism of HARF.

We only focus on the adorned tube and develop a plane transmission model by disassembling the HARF structure into several layers, as presented in Fig.2. When optical ray propagates in the core, the glancing angle (θ) would be limited to be a small value owing to the typical core size[21]. As shown in Fig.2(b), a single wave (indicated by the red arrows) first impinges on the silica/air interface, part of the light is reflected to the air core and the others is transmitted into the silica tube. The transmitted light will experience the same process on the silica/MIL interface with inequable optical transmissivity. Based on the Snell's law and Fresnel formula, the proportionality factor of the single-path light transmission from the air core to the silica tube can be obtained by[21]

$$\frac{I_s}{I} \approx 4\sin\theta \cdot \frac{1}{\sqrt{n_t^2-1}}, \tag{1}$$

$$\frac{I_p}{I} \approx 4\sin\theta \cdot \left(\frac{1}{\sqrt{n_t^2-1}} + \sqrt{n_t^2-1}\right), \tag{2}$$

where I_s is the energy of the transmitted ray for s-polarization, I_p is the energy of the transmitted ray for p-polarization, and the total incidence energy is $2I$. n_t is the RI of the silica tube. The optical transmissivity for single silica/air interface is $(I_s+I_p)/2I$, and it is easy to understand that the proportion of the single-path light transmission is an exponential function of the number of interfaces, if no medium is introduced into the tube. But on the other hand, the proportionality factor of the single-path light transmission from the silica tube to the intentionally introduced medium would be approximately derived to be

$$\frac{I_s'}{I_s} \approx \frac{4\sqrt{n_t^2-1}\cdot\sqrt{n_l^2-1}}{\left(\sqrt{n_t^2-1}+\sqrt{n_l^2-1}\right)^2}, \tag{3}$$

$$\frac{I_p'}{I_p} \approx \frac{4\sqrt{n_t^2-1}\cdot\sqrt{n_l^2-1}}{\left(\frac{n_l\sqrt{n_t^2-1}}{n_t}+\frac{n_t\sqrt{n_l^2-1}}{n_l}\right)^2}. \tag{4}$$

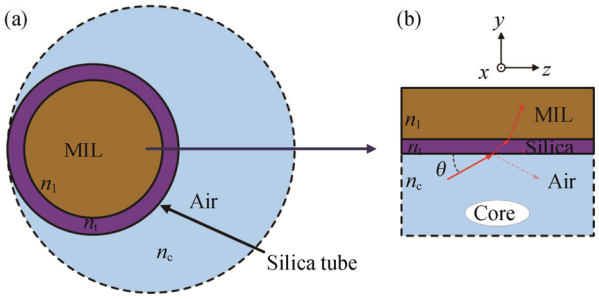

Fig.2 (a) Cross section of the adorned tube in HARF; (b) Two-dimensional plane transmission model

The derivation of the formulas is based on the initial condition: the glancing angle (θ) in the core is far less than 1, n_l is the RI of the introduced medium inside the tube. In order to exhibit the variation of the optical transmissivity around the silica/medium interface more visually, the optical transmissivities of s- and p-polarization as a function of the RI of medium is shown in Fig.3, when the RI of medium is getting damn close to the RI of air (i.e., $n_l \approx 1$), the optical transmissivities are both tiny for s- and p-polarization, and Eqs.(3) and (4) evolve to be Eqs.(1) and (2) analogously. While the optical transmissivity would increase with the medium index until $n_l=n_t$, and then decreases. Obviously, the optical transmissivities reach the maximum when $n_l=n_t$, which hints that the confinement loss (*CL*) of the HARF would be influenced by the introduced medium in comparison with the unadorned fiber.

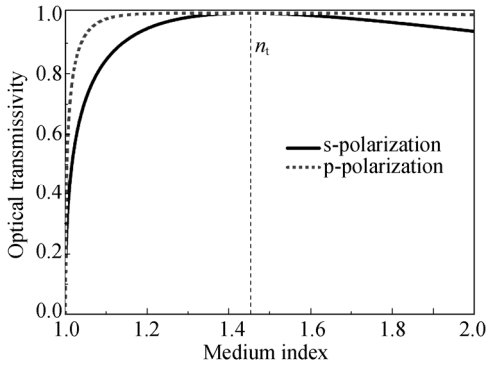

Fig.3 The optical transmissivities of s-polarization and p-polarization as a function of the RI of medium for the silica/material interface

MIL is considered as perturbation medium that allows for the leakage of light energy from the fiber core into the MIL. The optical leaky modes will then be absorbed and damped by the medium. Therefore, the adorned HARF structure could be employed to fabricate the *CL*-dependent fiber device. We define the mode-leakage-factor (MLF) to normalize the leaky mode energy in the liquid medium with respect to the overall light energy distributed over the cross sectional of the HARF by using the integral of Poynting vector for arbitrary polarization component. Considering that the leaky mode energy in the medium $i=\iint_M \boldsymbol{S}\cdot z\mathrm{d}x\mathrm{d}y$, and the overall energy distribution in the HARF $I=\iint_H \boldsymbol{S}\cdot z\mathrm{d}x\mathrm{d}y$, the MLF could be defined as

$$MLF=10\log_{10}\left(\frac{\iint_M \boldsymbol{S}\cdot z\mathrm{d}x\mathrm{d}y}{\iint_H \boldsymbol{S}\cdot z\mathrm{d}x\mathrm{d}y}\right). \tag{5}$$

According to Eq.(5), different amounts of adorned tubes would cause the change of MLF. In order to investigate the polarization performances of the HARFs with multifarious adorned tubes, we numerically simulate the energy profiles of the HARFs and calculate the MLF difference between the *x*-polarization and *y*-polarization components by using the finite element method (FEM), and the mentioned model in Fig.1 is shown to have the maximum MLF difference of 22.03 dB, which is optimal to serve as the fiber polarizer.

Fig.4 shows the *CL* ratio of the two orthogonal polarization components around 1 550 nm for the employed model. The mode field distributions of different polarization modes at 1 550 nm are shown in the inset of Fig.4. It is apparent that the light energy of the *x*-polarization mode is well confined in the core of the HARF, and the mode field distribution roughly maintains unchanged. However, the *y*-polarization mode acts as the leaky mode, which is quickly dampened in the MIL. Additionally, the simulated *CL* of the *x*-polarization mode is significantly lower than that of the *y*-polarization mode for the wavelength range of 1 535 nm to 1 565 nm. The above simulation results indicate that the proposed HARF could be employed as a fiber polarizer with high *PER*.

For most present fiber polarizers, the *PER*s could not be adjusted. A liquid-crystal-infiltrated photonic bandgap fiber polarizer is proposed by integrating the fiber structure in a double silicon v-groove assembly, and the *PER* could be electrically controlled[22]. Although the device presents excellent polarization performances, the device fabrication procedure is a bit complicated. In the above section, we built a plane transmission model to demonstrate the power leakage of the incident light from HARF core into the deliberately introduced medium. Numerical simulation indicates that most of the leaky mode derives from the *y*-polarization mode, which is the formation mechanism of the proposed polarizer. Here we investigate a new factor which may impact on the polarization performance of the polarizer, i.e. the absorption and scattering coefficients of the medium, which have almost not been discussed before. As is well known, the optical paths are reversible, in addition to the energy suffers from attenuation in medium, the remaining energy of the leaky ray may re-enter into the core, which provides a trajectory to regulate the polarization properties flexibly. Supposing that the absorption and scattering coefficients of the medium can be mutable under the action of external fields, the energy dissipation into the medium would increase accordingly. And afterwards, a *PER* adjustable all fiber polarizer could be derived by the efficient yet simple technique.

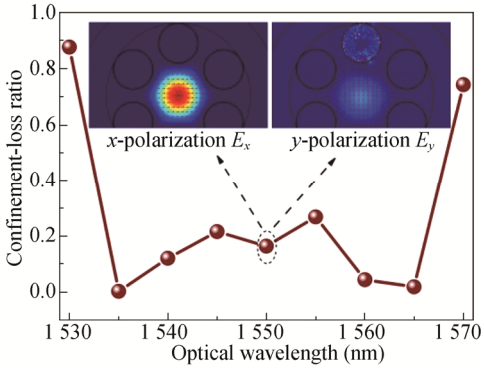

Fig.4 Calculated wavelength-dependent confinement-loss ratio for the two orthogonal polarization modes (Insets give the mode field distributions at 1 550 nm for the *x*-polarization and *y*-polarization modes, respectively.)

The sanguine medium employed in this letter is MIL, compared with the conventional IL, the local ordering of the anions under the external magnetic field is the most outstanding feature for MIL[23]. In principle, the amount of the magnetic anions participating in aligning locally will increase with the magnetic field intensity and the anion chains agglomerate towards the axis of the applied magnetic field. Spontaneously, the aligned anions become the new optical absorption and scattering centers, which would further increase the energy consumption of the leaky mode. The absorption and scattering coefficients (κ) of MIL under the external magnetic field can be defined as[24]

$$\kappa=\frac{2\pi}{\lambda'}\phi\left[\frac{4\pi\sigma/\omega}{\left[1+\langle N\rangle(\varepsilon-1)\right]^2}+\frac{4\pi^2\upsilon_0}{3\lambda'^3}\left[\frac{\varepsilon-1}{1+\langle N\rangle(\varepsilon-1)}\right]^2 m\right], \tag{6}$$

where $\lambda'=\lambda/\sqrt{\varepsilon_1}$, and ε_1, ϕ, σ, ω, ε, υ_0 are representative of the dielectric constant, volume fraction, electrical conductivity, angular frequency, relative dielectric constant and the volume of anion, respectively. Under a weak magnetic field, the aforementioned physical parameters almost remain on hold, whereas the mean depolarization factor $\langle N\rangle$ and the average number of anion in chains *m* will change with the magnetic field due to the formation of anion aggregates. The mean depolariza-

tion factor $\langle N\rangle = \phi^{-1}\sum_{k=0}^{\infty} k\upsilon_0\upsilon_k N_k$, where υ_k is the density of chains with k anions, the depolarization coefficient for a chain is N_k. Assuming the magnetic chain to be ellipsoid of rotation, and we can derive $N_k = \frac{1-e_r^2}{2e_r^3}(\ln\frac{1+e_r}{1-e_r} - 2e_r)$, where e_r is the eccentricity, and $e_r = \sqrt{1-\frac{1}{r^2}} = \sqrt{1-(\frac{a}{b})^2}$, a and b are the diameter and length of a chain, respectively. Demonstrably, the mean depolarization factor $\langle N\rangle$ would decrease with b growing and increase with a thickening. Considering the fact that the growing rate of b is faster than the thickening rate of a, the mean depolarization factor $\langle N\rangle$ would decrease with the magnetic field, while the average number of anion in chains m would increase synchronously. According to Eq.(6), the inverse variation of the variables, i.e., $\langle N\rangle$ and m would result eventually in the increase of the absorption and scattering coefficients κ. Accordingly, the *PER* of the MIL-adorned HARF polarizer will theoretically increase with the magnetic field.

For experimental demonstration, the structure parameters of the employed HARF are depicted in Fig.5, with an outer diameter of 144 μm, a core diameter of 40 μm, an inner diameter of the surrounding tube of 24 μm, and the thickness of the tube is about 410 nm. In order to implement the construction of the most efficient polarizer as noted above, a kind of polystyrene sphere with the diameter of 32 μm is employed to clog the desired cladding tube by a glass tip under the microscope, the polystyrene sphere is shown in Fig.5(a) and the overlayed tube is depicted in the red circle of Fig.5(b). Thanks to the low melting point and high remoldability of polystyrene, the polystyrene sphere is heated to block the tube thoroughly, as shown in Fig.5(c). Afterwards, a bit of molten paraffin is pumped into the single-tube-blocked HARF and then the HARF is cut to reopen the desired tube while keeping the others blocked by paraffin. After this is done, the MIL is infiltrated into the desired tube to adorn the HARF with a pressure pump. In experiment, the adorned HARF with a length of 9.5 cm is sandwiched between two single mode fibers (SMFs), in order to overcome the issue of the diameter mismatch of the two fibers, the splicing is achieved by the manual fusion technology. Note that a slight structural deformation of HARF which may also contribute to the *PER* is observed during the splicing for the delicate and fragile structure, despite the low discharge power and short discharging duration are programmed. Fig.5(d) shows the evolution of the wavelength-dependent *PER* for the original and adorned HARF, respectively. Apparently, the *PER* of the original HARF is extremely low while that will increase to 10 dB once the fiber is adorned by MIL. We define the 3 dB bandwidth to be the operation bandwidth of the polarizer, and the 3 dB bandwidth of the adorned HARF is approximately 24.5 nm over the wavelength range from 1 531.5 nm to 1 556 nm.

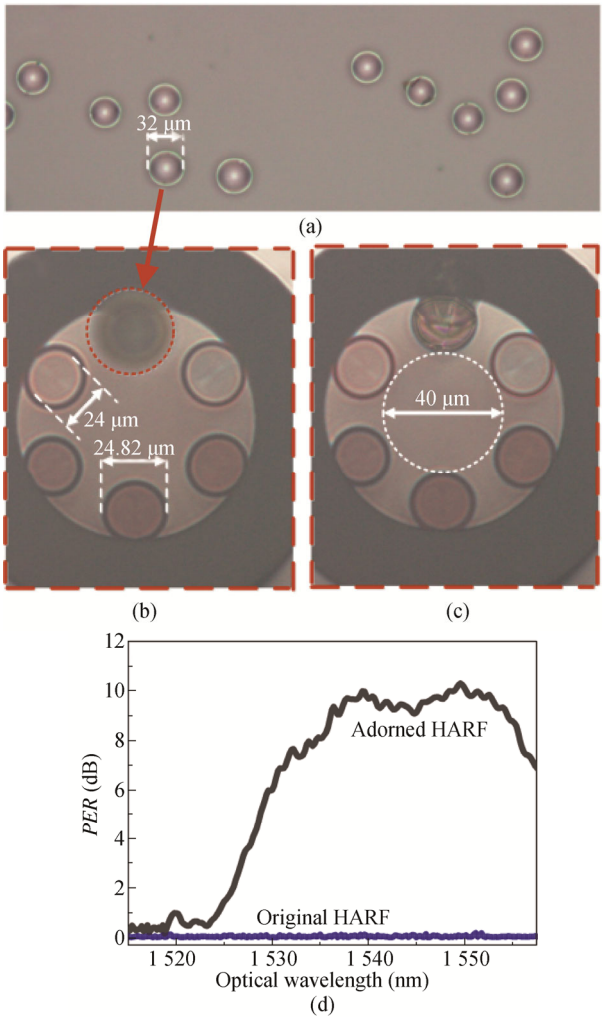

Fig.5 (a) The microscope image of the polystyrene sphere; (b) The cross section of the polystyrene-sphere-overlayed HARF; (c) The molten polystyrene sphere; (d) Evolution of the *PER* for original and adorned HARF

The wavelength-dependent *PER*s of the HARF under different intensity of magnetic field are exhibited in Fig.6(a), the *PER* increases with the magnetic field, which is coincide with the theoretical analysis and the *PER* increases to 18.5 dB under the magnetic field intensity of 400 Oe. We trace the *PER* shift of the polarizer at the wavelength of 1 550 nm, as shown in Fig.6(b), from 0 Oe to 100 Oe, the *PER* varies slightly owing to the effect of the initial magnetization of MIL, which is similar to the magnetic fluid[25,26]. As the magnetic field intensity increases to 350 Oe, almost all of the anions are agglomerated to form the magnetic chains with fixed arrangement, and the MIL reaches its saturation magnetization state ultimately, which cause the fluctuation of the *PER* as the magnetic field increases from 350 Oe to 400 Oe. However, for the range of 100 Oe~350 Oe, the *PER* shift varies linearly with the sensitivity of 0.032 47 dB/Oe. In addition, the 3 dB bandwidth change of the polarizer under applied magnetic field has been investigated as well, and the variation is less than 1 nm,

which may be attributed to the tiny RI change of MIL.

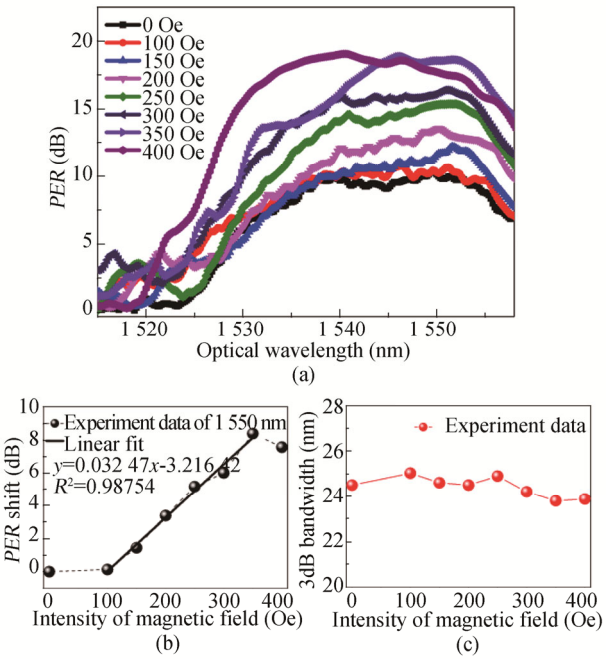

Fig.6 (a) Evolution of the *PER* with the increment of magnetic field; (b) *PER* shift for the wavelength of 1 550 nm as functions of applied magnetic field intensity; (c) 3 dB bandwidth variation for the polarizer under different magnetic field

As a fiber optical device, the thermostability is an important factor to judge the polarizer's capability. The temperature-dependent *PER* is depicted in Fig.7, and the temperature is demonstrated to have little impact on the *PER* of the polarizer, the *PER* variation for the wavelength of 1 550 nm is less than 0.8 dB and the reason for this is that the mean depolarization factor $\langle N \rangle$ and the average number of anion in chains *m* are virtually impervious to temperature. However, very interestingly, the 3 dB bandwidth of the polarizer would vary with the temperature obviously, which is most likely due to the temperature-induced RI decrease for MIL. According to the inset of Fig.7, as the temperature increases from 25 °C to 45 °C, the 3 dB bandwidth increases from 23.5 nm to 33.1 nm accordingly.

By introducing the local RI contrast into the HARF to modulate the single-path Fresnel transmission, a fiber polarizer could be derived. The theoretical modeling and experimental demonstration could help us further understand the optical guidance mechanism of HARF and optimize the performance of the polarizer, such as adjusting the RI of material or the length of the MIL-adorned section. Furthermore, the aforementioned structural deformation of HARF during the splicing can enhance the waveguide asymmetry and may be likely to contribute to the *PER*, which obviously deserves further studies for additional performance boost.

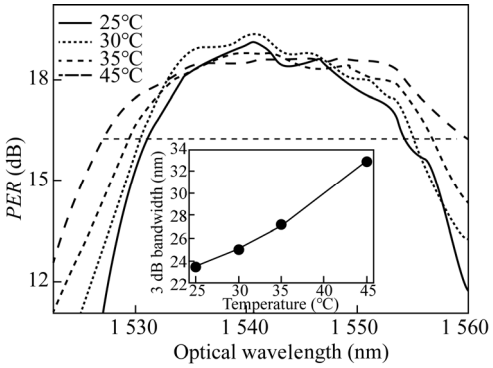

Fig.7 Temperature dependence of *PER* for the polarizer, where inset is the 3 dB bandwidth variation under different temperature

In conclusion, this paper exhibits a magnetically driven HARF polarizer. We introduce a plane transmission model that approximates the light leakage in an MIL-adorned HARF, comparison with numerical simulation confirm the selective conversion between the polarization mode and leaky mode and the polarizing effect originates from the different attenuation of the orthogonal modes. Owing to the controllable optical absorption and scattering coefficients of MIL, the *PER* can increase from 10 dB to 18.5 dB with the increment of magnetic field. Our demonstration offers a potential way to clarify the light confinement in HARF and may arrest more attentions to expand the application field of HARF.

References

[1] X. S. Yao, H. F. Xuan, X. J. Chen, H. H. Zou, X. Liu and X. Zhao, Opt. Express **27**, 19984 (2019).

[2] R. B. Dyott, J. Bello and V. A. Handerek, Opt. Lett. **12**, 287 (1987).

[3] S. M. Tseng, K. Y. Hsu, H. S. Wei and K. F. Chen, IEEE Photon. Technol. Lett. **9**, 628 (1997).

[4] Y. P. Wang, L. M. Xiao, D. N. Wang and W. Jin," Opt. Lett. **32**, 1035 (2007).

[5] H. F. Xuan, W. Jin, J. Ju, L. Y. P. Wang, M. Zhang, Y. B. Liao and M. H. Chen, Opt. Lett. **33**, 845 (2008).

[6] Z. J. Yan, K. M. Zhou and L. Zhang, Opt. Lett. **37**, 3819 (2012).

[7] C. H. Dong, C. L. Zou, X. F. Ren, G. C. Guo and F. W. Sun, Appl. Phys. Lett. **100**, 041104 (2012).

[8] Y. B. Lin, J. P. Guo and R. G. Lindquist, Opt. Express **17**, 17849 (2009).

[9] X. B. Zheng, Y. G. Liu, Z. Wang, T. T. Han and B. Y. Tai, IEEE Photon. Technol. Lett. **23**, 709 (2011).

[10] W. W. Qian, C. L. Zhao, Y. P. Wang, C. C. Chan, S. J. Liu and W. Jin, Opt. Lett. **36**, 3296 (2011).

[11] N. M. Litchinitser, S. C. Dunn, P. E. Steinvurzel, B. J. Eggleton, T. P. White, R. C. Mcphedran and C. M. D. Sterke, Opt. Express **12**, 1540 (2004).

[12] C. L. Wei, C. R. Menyuk and J. Hu, Opt. Express **24**, 12228 (2016).

[13] M. S. Habib, J. E. Antoniolopez, C. Markos, A. Schulzgen and R. Amezcuacorrea, Opt. Express **27**, 3824

(2019).
[14] P. Jaworski, F. Yu, R. R. J. Maier, W. J. Wadsworth, J. C. Knight, J. D. Shephard and D. P. Hand, Opt. Express **21**, 22742 (2013).
[15] U. Elu, M. Baudisch, H. Pires, F. Tani, M. H. Frosz, F. Kottig, A. Ermolov, P. S. Russell and J. Biegert, Optica **4**, 1024 (2017).
[16] F. Kottig, F. Tani, C. M. Biersach, J. C. Travers and P. S. Russell, Optica **4**, 1272 (2017).
[17] M. R. A. Hassan, F. Yu, W. J. Wadsworth and J. C. Knight, Optica **3**, 218 (2016).
[18] J. R. Hayes, S. R. Sandoghchi, T. D. Bradley, Z. X. Liu, R. Slavik, M. A. Gouveia, N. V. Wheeler, G. Jasion, Y. Chen, E. N. Fokoua, M. N. Petrovich, D. J. Richardson and F. Poletti, J. Lightwave Technol. **35**, 437 (2017).
[19] X. L. Liu, W. Ding, Y. Y. Wang, S. F. Gao, L. Cao, X. Feng and P. Wang, Opt. Lett. **42**, 863 (2017).
[20] M. Zeisberger and M. A. Schmidt, Sci. Rep. **7**, 11761 (2017).
[21] Y. Y. Wang and W. Ding, Opt. Express **25**, 33122 (2017).
[22] T. T. Alkeskjold and A. Bjarklev, Opt. Lett. **32**, 1707 (2007).
[23] S. Hayashi, S. Saha and H. Hamaguchi, IEEE T. Magn. **42**, 12 (2006).
[24] V. Socoliuc, M. Rasa, V. Sofonea, D. Bica, L. Osvath and D. Luca, J. Magn. Magn. Mater. **191**, 241 (1999).
[25] Yuan Gao, Bicheng Dong, Ce Tan, Yan Wang, Haosheng Zhu and Hai Liu, Journal of Optoelectronics·Laser **28**, 1344 (2017). (in Chinese)
[26] Fuquan Shi, Yan Luo, Jiajia Chen and Baojin Peng, Journal of Optoelectronics·Laser **28**, 1290 (2017). (in Chinese)